IOPscience iopscience.iop.org

Home Search Collections Journals About Contact us My IOPscience

The effects of the intense laser and homogeneous electric fields on the electronic and intraband optical properties of a GaAs/$Ga_{0.7}Al_{0.3}$As quantum ring

This content has been downloaded from IOPscience. Please scroll down to see the full text.

2015 Semicond. Sci. Technol. 30 045006

(http://iopscience.iop.org/0268-1242/30/4/045006)

View the table of contents for this issue, or go to the journal homepage for more

Download details:

IP Address: 130.209.115.82
This content was downloaded on 21/10/2015 at 12:04

Please note that terms and conditions apply.

OPEN ACCESS
Made open access 28 July 2015
IOP Publishing
Semiconductor Science and Technology
Semicond. Sci. Technol. **30** (2015) 045006 (9pp)
doi:10.1088/0268-1242/30/4/045006

The effects of the intense laser and homogeneous electric fields on the electronic and intraband optical properties of a GaAs/$Ga_{0.7}$ $Al_{0.3}$As quantum ring

A Radu[1], **A A Kirakosyan**[2], **D Laroze**[3,4] **and M G Barseghyan**[2,5]

[1] Department of Physics, Politehnica University of Bucharest, 313 Splaiul Independentei, Bucharest RO-060042, Romania
[2] Department of Solid State Physics, Yerevan State University, Alex Manoogian 1, 0025 Yerevan, Armenia
[3] Instituto de Alta Investigación, Universidad de Tarapacá, Casilla 7D, Arica, Chile
[4] SUPA School of Physics and Astronomy, University of Glasgow, Glasgow G12 8QQ, UK
[5] National University of Architecture and Construction of Armenia, Teryan 105, 0009 Yerevan, Armenia

E-mail: mbarsegh@ysu.am

Received 12 September 2014, revised 1 February 2015
Accepted for publication 17 February 2015
Published 11 March 2015

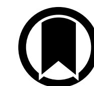

Abstract

The simultaneous influences of an intense laser field and static electric field on one-electron states and intraband optical absorption coefficient are investigated in two-dimensional GaAs/Ga $_{0.7}Al_{0.3}$ As quantum ring. An analytical expression of the effective confining potential in the presence of the external fields is obtained. The one-electron energy levels and wave functions are calculated using the effective mass approximation and an exact diagonalization technique. We show that changes in the incident light polarization lead to blue- or redshifts in the intraband optical absorption spectrum. Moreover, we found that blueshift and redshift are induced by the simultaneous influences of an intense laser and lateral electric fields. The obtained theoretical results indicate a novel opportunity to tune the performance of quantum rings and to control their specific properties by means of intense laser and homogeneous electric fields.

Keywords: quantum ring, laser field, electric field

(Some figures may appear in colour only in the online journal)

1. Introduction

Quantum mechanical experiments in ring-like geometries have long fascinated the physics community, as electrons confined in nanometric rings manifest a topological quantum mechanical coherence, the Aharonov–Bohm effect [1]. Unlike quantum dots (QDs) the ground state total angular momentum in QR changes from zero to nonzero value by increasing the magnetic field [2, 3]. With the developments in nanotechnology, the formation of different types of semiconductor QRs is now possible [4, 5]. Most of the experimental work is based on self-assembled QRs made of InAs quantum dots capped with a thin GaAs layer subjected to a short (but crucial) annealing, but also lithographic techniques have been used for the fabrication of InGaAs QRs [6]. The self-assembling of non-III–V semiconductor QRs of SiGe has been achieved, too [7]. The tendency toward enlargement of the semiconductor QRs family in the nearest future is quite clear by now. Note that many studies revealed great potentialities of QRs as basis elements for a broad spectrum of applications, starting from terahertz detectors [8], efficient solar cells [9] and memory devices [10], through electrically tunable optical valves and single photon emitters [11], and further to spin qubits for quantum computing [12].

In the past few years, the development of modern high-power, tunable laser sources, e.g. free-electron lasers, has

Content from this work may be used under the terms of the Creative Commons Attribution 3.0 licence. Any further distribution of this work must maintain attribution to the author(s) and the title of the work, journal citation and DOI.

allowed the experimental study of the interaction of intense laser fields (ILFs) with charge carriers in semiconductors, mainly in the terahertz frequency range [13–15]. Interestingly, by illuminating nanostructures with ILFs some new physical phenomena were theoretically anticipated and observed. We can mention, for instance, terahertz resonant absorption [16], strong distortions in the optical absorption spectra [17], and Floquet–Bloch states in single-walled carbon nanotubes [18].

On the other hand, the characteristic wavelengths determined by the position of the energy levels are very important in many applications. One way to change the position of the levels is to tailor the size of the nanostructures. However, for a given structure the transition energy between two levels is almost fixed (neglecting the fluctuations of temperature and external hydrostatic pressure) in the absence of external fields. An externally applied electric field alters the potential energy profile of the structure and accordingly the positions of the energy levels.

In the past decade a large number of theoretical investigations were devoted to the study of electronic and impurity states and intraband optical properties in nanostructures under the simultaneous influence of ILF and external electric field. The effect of the high-frequency laser field on the intersubband optical absorption in a quantum well (QW) heterostructure in the presence of an external electric field was studied in [19]. The ILF, electric field, and the geometric confinement effects on the intersubband absorption coefficient in a double-graded QW were investigated in [20]. The effect of the ILF on the nonlinear optical properties of a square QW under the applied electric field were studied in [21]. In [22], based on the effective-mass approximation, the competition effects between the ILF and applied electric field on impurity states were investigated in the GaN/AlGaN QW. The combined effects of intense laser field and applied electric field on the nonlinear optical absorption and refractive index change in $Ga_{1-x}Al_xAs$/GaAS single QW [23] and $Ga_{1-x}In_xN_yAs_{1-y}$/GaAs double QWs [24] were reported within the framework of the compact density matrix approach and iterative method. The effect of the ILF on the optical absorption coefficients and the refractive index changes in a GaAs/GaAlAs parabolic quantum well under the applied electric field were investigated in [25]. In [26] the laser-field dependence of the impurity binding energy and the donor-related photoionization cross-section in a graded quantum-well wire (QWW) under an external static electric field were calculated by a variational method and in the effective mass approximation. Based on the effective-mass approximation, the effects of external electric field and ILF on the binding energy of an on-center hydrogenic donor impurity in a spherical QD embedded in a cylindrical nano-wire was studied in [27]. Using the effective mass and parabolic band approximations and a variational procedure Duque *et al* calculated the combined effects of intense laser radiation, hydrostatic pressure, and applied electric field on a shallow-donor impurity states confined in cylindrical-shaped single and double GaAs/$Ga_{1-x}Al_xAs$ QD [28]. Using a perturbative method, Burileanu has investigated the behavior of the binding energy and photoionization cross-section of a donor impurity in spherical QD under the influence of electric and laser fields [29]. The ILF effect on the impurity states in a CdS/SiO_2 QD under applied electric field was studied within the effective massapproximation by using a finite difference method [30].

Note that, in our previous work [31] the influence of intense laser field on one-electron states and intraband optical absorption were investigated in two-dimensional GaAs/$Ga_{0.7}Al_{0.3}$As QR. Our results showed that the change of the incident light polarization direction can induce red and blue shifts in the absorption spectrum of the quantum ring. We have also found that only blueshift is obtained with the increasing of outer radius of the QR.

Having this motivation, the present work aims at the theoretical investigation of the combined influences of the ILF and lateral electric field (electric field direction is contained in the plane of the structure) on one-electron states and intraband optical absorption coefficient of GaAs/$Ga_{0.7}Al_{0.3}$As two-dimensional QR. The paper is organized as follows. In section 2 we describe the theoretical framework. Section 3 is dedicated to the results and discussion, and our conclusions are given in section 4.

2. Theoretical framework

We consider a cylindrical GaAs QR surrounded in the radial direction by a material with a larger energy gap, such as $Al_xGa_{1-x}As$. Usually, the thickness of the ring along the growth direction is much smaller than the radial dimensions. Consequently, without loss of generality, our system can be considered two-dimensional, with the electron confined in the plane $z = 0$ [32, 33]. For the lateral confining potential we have taken a finite, square-type well

$$V(x\mathbf{i} + y\mathbf{j}) = \begin{cases} 0, & \textit{if } R_1 \leqslant \sqrt{x^2 + y^2} \leqslant R_2, \\ V_0, & \textit{if} \sqrt{x^2 + y^2} < R_1, \textit{or} \sqrt{x^2 + y^2} > R_2. \end{cases} \quad (1)$$

where $\mathbf{i}$ and $\mathbf{j}$ are the unit vectors along the laser polarization and the y- axis respectively, R_1 and R_2 are the inner and outer radii of the QR, respectively, and V_0 is the conduction band offset.

We assume the system to be under the action of laser radiation represented by a monochromatic plane wave of frequency ω_0, and external lateral electric field. We choose the electric field oriented along the x- axis. The laser beam is non-resonant with the semiconductor structure, and linearly polarized along a radial direction of the QR, chosen as the direction of the electric field. In the high-frequency regime the particle is subjected to the time-averaged potential [34, 35]

$$V_d(x, y) = \frac{\omega_0}{2\pi} \int_0^{2\pi/\omega_0} V\left(\left(x + \alpha_0 \, sin\,(\omega_0 t)\right)\mathbf{i} + y\mathbf{j}\right) dt \quad (2)$$

where $\alpha_0 = eA_0/(m\omega_0)$ denotes the laser field parameter, m- is the electron effective mass, and $\mathbf{A_0} = A_0\mathbf{i}$ is the vector potential.

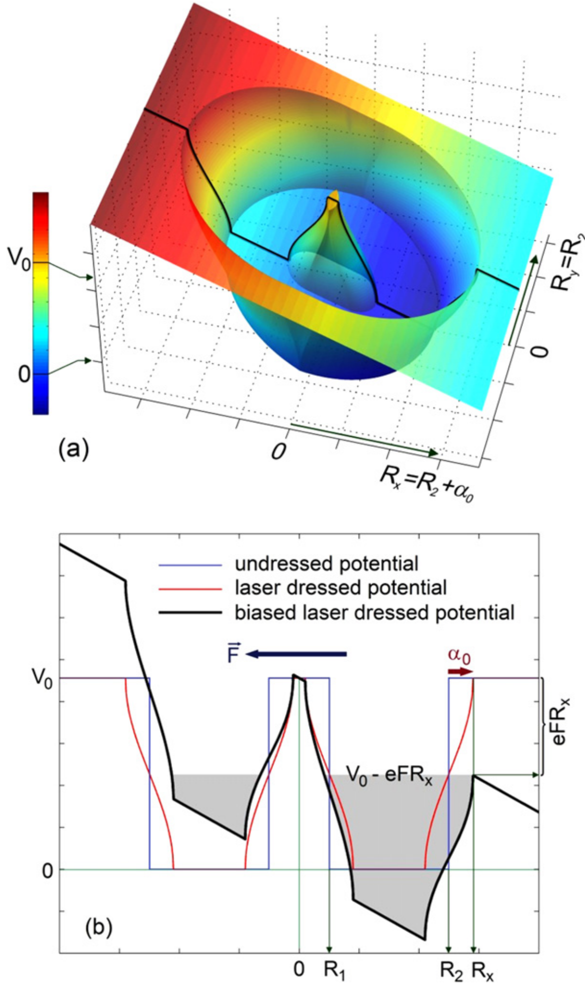

Figure 1. (a) Confinement potential of the QR modified by simultaneous actions of the laser and electric fields. The effective radius R_x in the field direction depends on the laser field parameter. (b) Axial section of the confinement potential along the x- axis. The grey area symbolizes the 'stability zone' of the electron bound states.

Taking into account equations (1) and (2)one may obtain a closed analytical form of $V_d(x, y)$, as in [31]. Taking for simplicity the same effective mass of the electron inside and outside the QR under electric field, the laser-dressed energies are obtained from the time-independent Schrödinger equation [36–38]

$$\left[-\frac{\hbar^2}{2\,m}\left(\frac{\partial^2}{\partial x^2}+\frac{\partial^2}{\partial y^2}\right) + V_d(x, y) - eFx\right]\Phi_d(x, y) = E_d\Phi_d(x, y). \quad (3)$$

The laser-dressed energy eigenvalues E_d^j and eigenfunctions $\Phi_d^j(x, y)$ may be calculated by solving equation (3) with a 2D diagonalization technique [39]. The eigenfunctions $\Phi_d^j(x, y)$ are presented as a linear expansion of the eigenfunctions of the rectangle with dimensions $L_x \times L_y$ and quantum numbers (n, m) [40–42].

Calculations of the optical absorption coefficient are based on Fermi's golden rule. The intraband absorbtion coefficient can be written as [43]

$$\alpha(\hbar\,\omega) = \frac{16\,\pi^2\,\beta_{FS}\hbar\,\omega}{n_r V}N_{if}\,\left|M_{fi}\right|^2\,\delta\left(E_f - E_i - \hbar\omega\right), \quad (4)$$

where n_r is the refractive index of the semiconductor, V is the volume of the sample per QR (in this work $V = 6\cdot 10^{-18}$ cm^3 [2]), β_{FS} is the fine structure constant, and $\hbar\omega$ is the incident photon energy, E_f and E_i are the energies of the final and initial states, respectively. Finally, $N_{if} = N_i - N_f$ is the difference of the numbers of electrons in the initial and final states. Since we consider here only a one particle problem, we have taken $N_i = 1$ for the ground state and $N_f = 0$ for all upper states. In equation(4) M_{fi} is the matrix element of the dipole operator [44]. We calculate the dipole matrix elements for x- and y-polarizations of the incident light and substituted the δ- function by a Lorentzian profile with the full width at half maximum of 0.8 meV.

3. Results and discussion

The calculations are performed for a GaAs/ $Ga_{0.7}Al_{0.3}As$ QR with parameter values $V_0 = 228$ meV, $n_r = 3.6$, $m = 0.067m_0$, where m_0 is the free-electron mass [45]. Note that, the photon energy $\hbar\omega_0$ of dressing laser must be much higher than the considered intraband transition energies such as the high-frequency dressing model to apply (~35 meV in our paper) but smaller than the energy barrier of the confinement such as the electron to remain confined and also no interband absorption to occur. This means that the laser frequency should be much higher than ~10 THz and lower than ~70 THz.

It should be recalled that for any finite barrier potential well under the action of an electric field there is no veritable electron bound state. Every energy level associated with a quantum state has a non-zero linewidth correlated with the mean time of tunneling out of the biased structure [46]. As the static electric field increases, the electron energies descend (quantum confined Stark effect), the tunneling time of a given state becomes smaller and the energy linewidth of the level augments [47]. However, this could be a real theoretical problem only for highly excited states which will become unsteady at high enough values of the electric field. The lower electronic states are quasi-bound since the associated tunneling time is much longer than any characteristic time involved in the intraband or interband transitions [46]. In this work we will not discuss this issue in more details but we will further establish a simple criterion for considering an excited state as being 'quasi-bound'.

Figure 1 presents the biased laser-dressed confinement potential of the QR. As is observable from figure 1(a) the dressing laser field 'stretches' the potential well on the x-

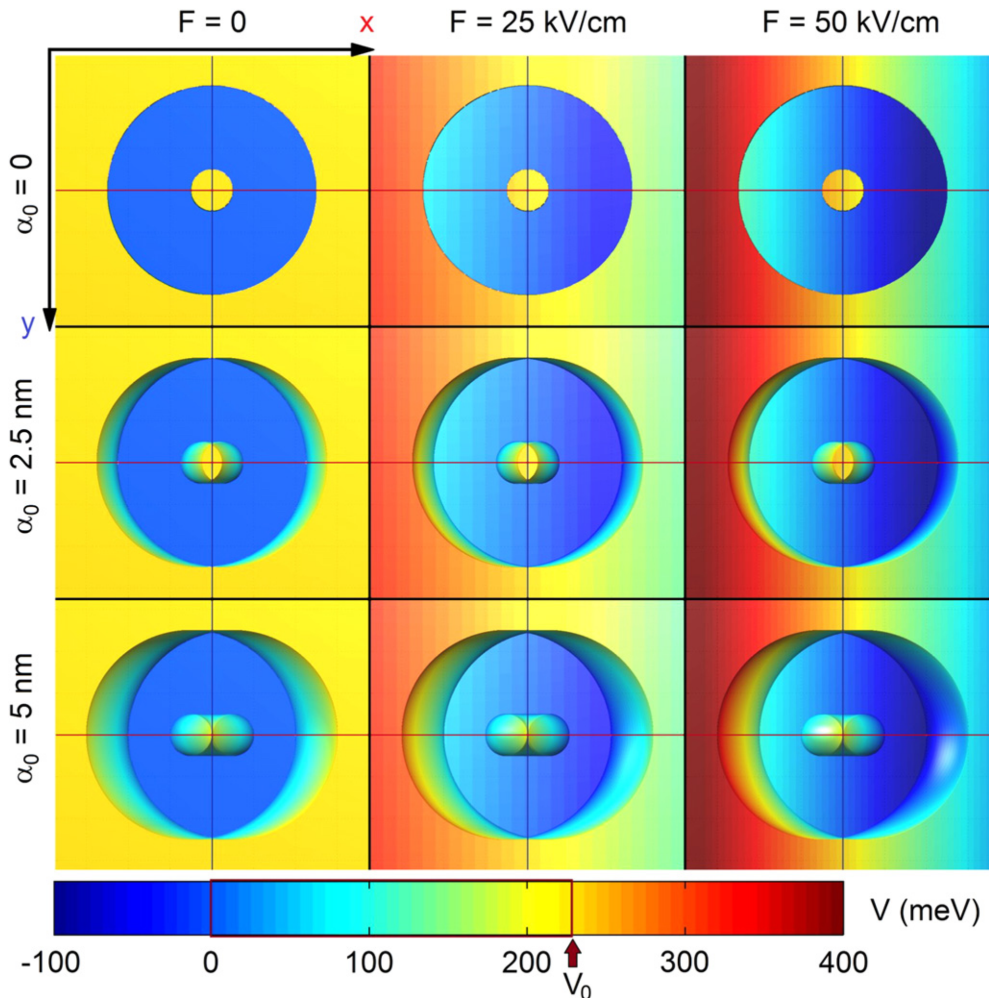

Figure 2. Density plot of the confinement potential of the QR modified by laser and electric fields.

direction at the same time as the collinear electric field 'tilts' the potential well on the same axis. Let us further consider as the 'interior' of the unbiased dressed potential well all points having the potential smaller than V_0. We will denote by R_x and R_y the 'effective radii' (the effective radius is defined as the half of the maximum confinement length on some particular direction) of the potential well on the fields' direction x and on the transverse direction y, respectively. Figure 1(b) shows the confinement potential as a function of x along the section $y = 0$. One may observe that the right edge of the potential well at $R_x = R_2 + \alpha_0$ is the lowest point of the confinement zone. Our approximate criterion of energy level stability will be based on the assumption that any electronic state j in the well whose energy E_d^j is still far below the lowest point of confinement may be considered as 'quasi-bound': $E_d^j \ll V_0 - eF(R_2 + \alpha_0)$. As an example, for $R_2 = 25$ nm, and $\alpha_0 = 5$ nm the lowest energy of confinement is 78 meV. In this case only excited states with considerably smaller energies should be considered in the calculations.

In figure 2 we present the colored surface of the QR's confinement potential which is modified by the simultaneous actions of the laser and electric fields. The dimensions of the QR are fixed $R_1 = 5$ nm and $R_2 = 25$ nm. The color scaling is determined by the value of the potential in each point. For a fixed barrier thickness the shape of the potential, that affects the carrier confinement, significantly changes in the presence of the laser field. With the increase of the laser field the effective length of the confining potential along the laser field polarization (x- direction) decreases in the lower part of the QR potential well. On the other hand, with the increase of the electric field the 'tilt' of the confinement potential increases. As a consequence, both fields destroy the cylindrical symmetry of the confinement potential.

In figure 3 the dependences of the first three undressed energy levels of the confined electron on the electric field strength F are presented. It should be mentioned that in the absence of both fields the excited state is twice degenerated. The electric field (laser field also, see figure 4(a)) removes this degeneracy as a result of broken axial symmetry. With the increase of the electric field strength, the ground state energy always decreases due to lowering of the bottom of the confinement potential, which is the analogue of the quantum confined Stark effect in quantum wells [48].

In figure 4(a)–(c) the dependences of first three dressed energy levels of the confined electron on the laser field parameter α_0 are presented for different values of electric field

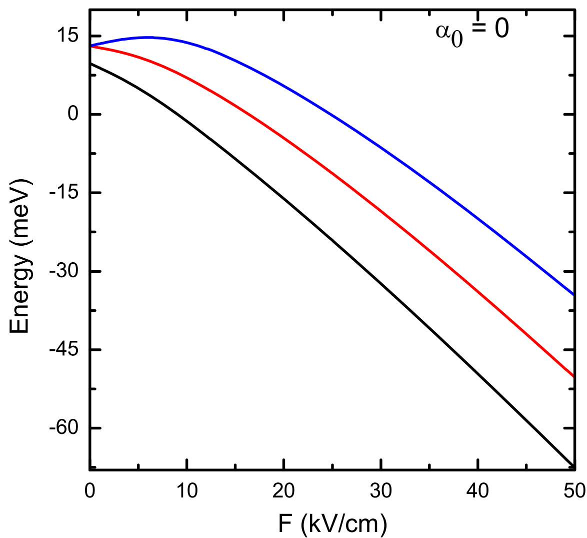

Figure 3. The first three undressed ($\alpha_0 = 0$) energy levels of the electron as function of the electric field strength F. The results are presented for $R_1 = 5$ nm and $R_2 = 25$ nm.

strength F. It should be mentioned that with the increase of the laser field the effective length (the dressing effect of the laser 'reshape' the confinement potential by enlarging the QR) of the confinement potential (for low lying states) along the laser field polarization (x-direction) decreases. For this reason, in all investigated cases the laser field brings to the increment of the dressed energies. On the other hand, in all regions of the laser field parameter variation the increment of the electric field strength moves the energy levels down, as was expected. Also, it is worth noting that the influence of the laser field on the ground state energy is stronger for bigger values of the electric field strength. To explain the above-mentioned effect in figure 5 we present the wave functions of the first three dressed stated of the electron (j = 1, 2, 3) as functions of the laser field parameter and electric field strength. If we compare ground state wave functions with no laser field in two cases: $F = 0$ (left panel below) and $F = 30\,\text{kV cm}^{-1}$ (right panel below), we clearly see that the effect of the electric field on the electron distribution in the structure is equivalent to an increasing of the spatial confinement. At $F = 0$, the localization probability will be uniformly distributed in the ring and the electron will be 'less confined'. At F = $30\,\text{kV cm}^{-1}$, the electron will be strongly 'pushed' against the right side of the QR and will be much 'more confined'. So it is a supplementary spatial confinement induced by the electric field. For example, in the case with $F = 0$, an increase in the laser field parameter from 0 to 5 nm produces an increase of the ground state energy of 3.3 meV, while in the case with $F = 15\,\text{kV cm}^{-1}$ and $F = 30\,\text{kV cm}^{-1}$ the ground state energies changes are 9.3 meV and 10.4 meV, respectively.

As seen in figure 5 for $F = 0$, the laser dressing radiation breaks down the polar symmetry of the wave function in the ground state. In the same time, the peaks of the wave function for $j = 2$ and $j = 3$ become exactly located along y- and x-axis, respectively. The first two excited states will correspond

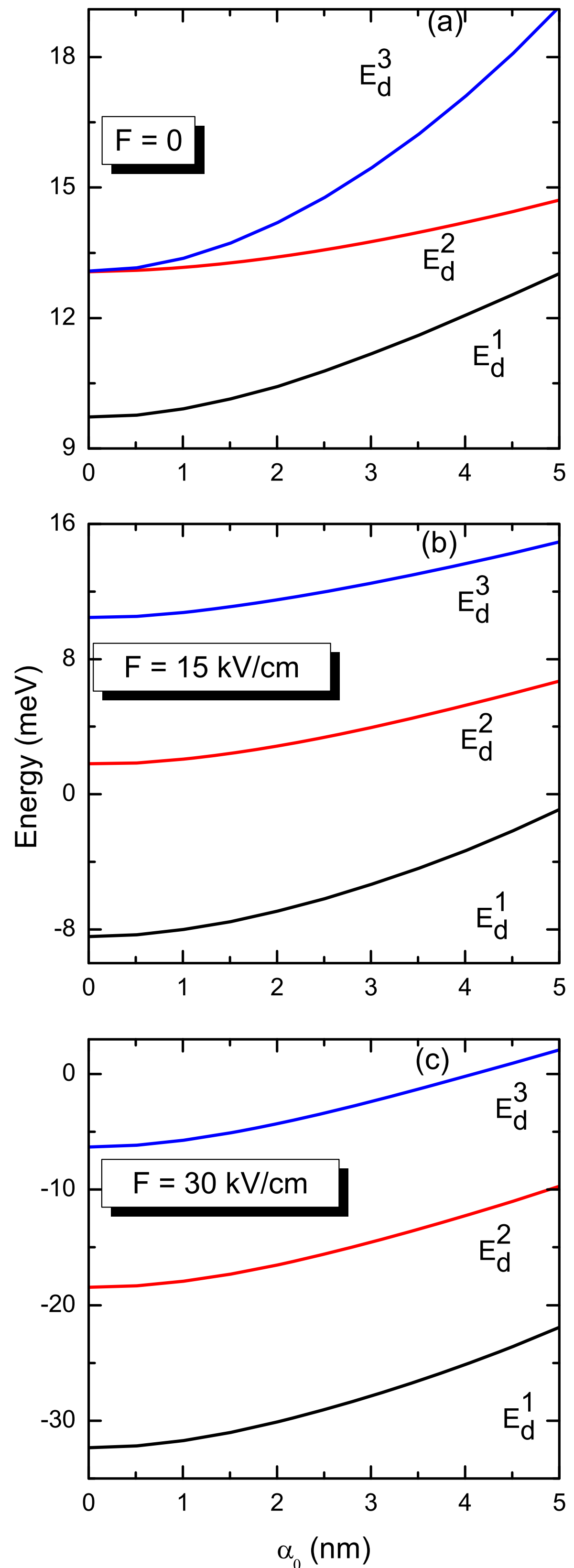

Figure 4. The first three dressed energy levels of the electron as function of the laser field parameter α_0. The results are presented for $R_1 = 5$ nm and $R_2 = 25$ nm. Several values of the electric field strength F are considered.

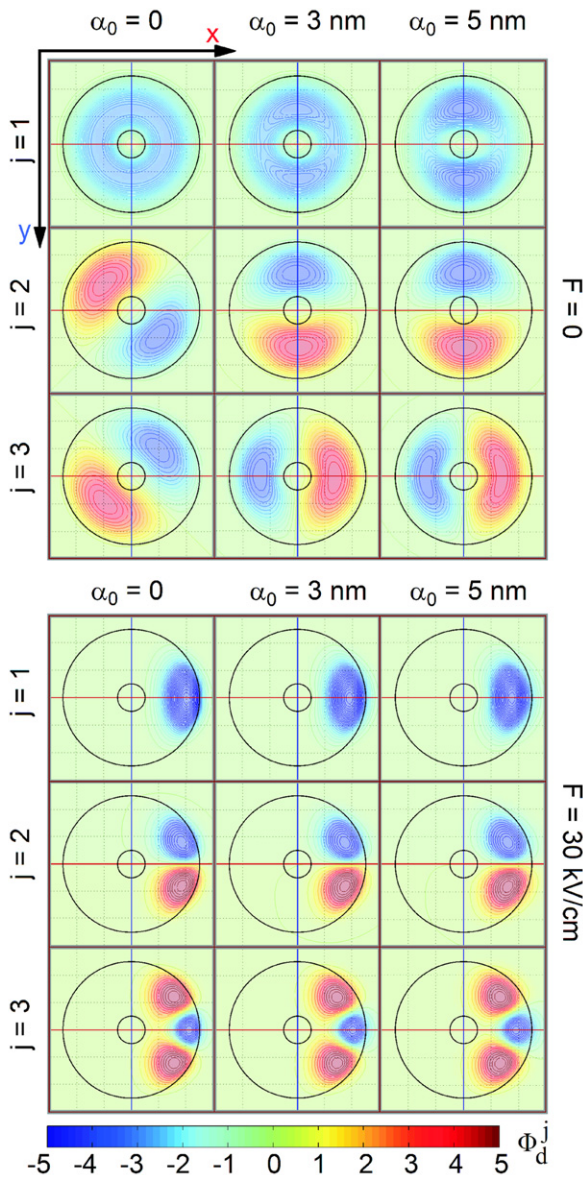

Figure 5. The wave functions of the first three dressed states of the electron (j = 1, 2, 3) as depending on the laser field parameter and electric field strength. The results are presented for R_1 = 5 nm and R_2 = 25 nm. Three values of the laser parameter (0, 3, 5 nm) and two values of the electric field strength (0, 30 kV cm^{-1}) are considered.

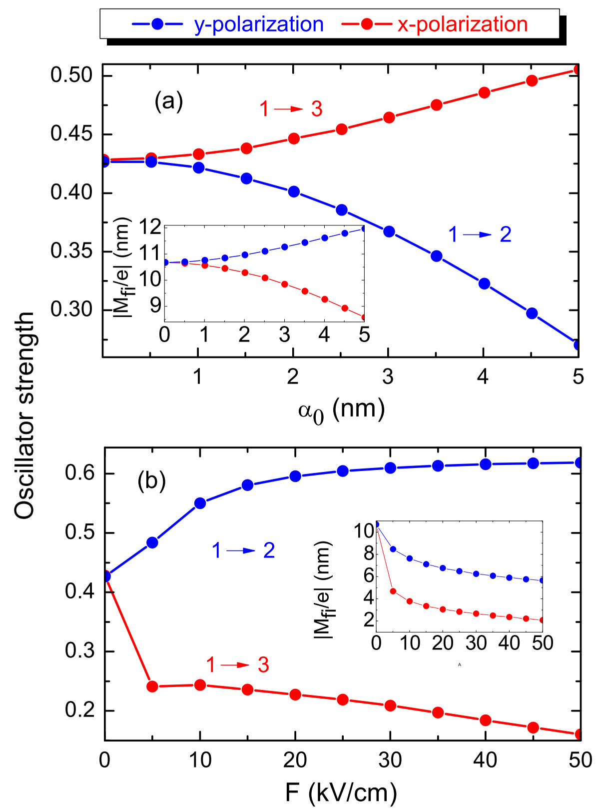

Figure 6. Oscillator strength as a function of laser field parameter (with F = 0) and electric field strength (with α_0 = 0), respectively. Figure insets show the absolute value of the matrix elements $|M_{fi}/e|$ as functions of the laser field parameter and electric field strength. The results are presented for R_1 = 5 nm and R_2 = 25 nm. Different light polarizations are considered.

to different energies, since the original degeneracy $E_2 = E_3$ was lifted by the laser field. So the laser field polarized on x-axis creates a radial anisotropy which is manifest by the two-fold splitting of the first excited state for no laser. In the presence of the electric field (lower half of figure 5), there is no degenerate state, even in the absence of the laser dressing. For all the first three states, the peaks of the electronic wave function are forced to locate in the QR in the lower part of the confinement potential (see figures 1 and 2). This is clearly visible in figure 5 where the localization probability is almost zero in the left part of the QR, for j = 1, 2, 3. The further increasing of the laser parameter has little effect on the wave function spatial configuration, but its effect is visible on the energies.

Let us now express the symmetry of the WFs in terms of two-variables function parity

- for $\alpha_0 = 0$ and $F = 0$ the ground and the excited, double-degenerate, states have both defined parity wave functions with respect to any direction in the QR plane (ground state is even, excited state is odd);

- for $\alpha_0 > 0$ and $F = 0$ the polar symmetry is reduced down to Cartesian symmetry with respect to $x-$ polarization of the laser field and transverse $y-$ axis: $\Phi_d^1(-x, y) = \Phi_d^1(x, y)$, $\Phi_d^1(x, -y) = \Phi_d^1(x, y)$, $\Phi_d^2(-x, y) = \Phi_d^2(x, y)$, $\Phi_d^2(x, -y) = -\Phi_d^2(x, y)$, $\Phi_d^3(-x, y) = -\Phi_d^3(x, y)$, $\Phi_d^3(x, -y) = \Phi_d^3(x, y)$;

- for $F > 0$ there is no symmetry with respect to the $y-$ axis, so there will be no defined parity of the wave functions in x variable; first and third states will have even wave functions in y variable while second state will have an odd wave function in y: $\Phi_d^1(x, -y) = \Phi_d^1(x, y)$, $\Phi_d^2(x, -y) = -\Phi_d^1(x, y)$, $\Phi_d^3(x, -y) = \Phi_d^3(x, y)$.

It is well known that the oscillator strength is an important physical quantity in the investigation of the optical properties which are related to the electronic dipole-allowed transitions, and it is a dimensionless quantity. The oscillator

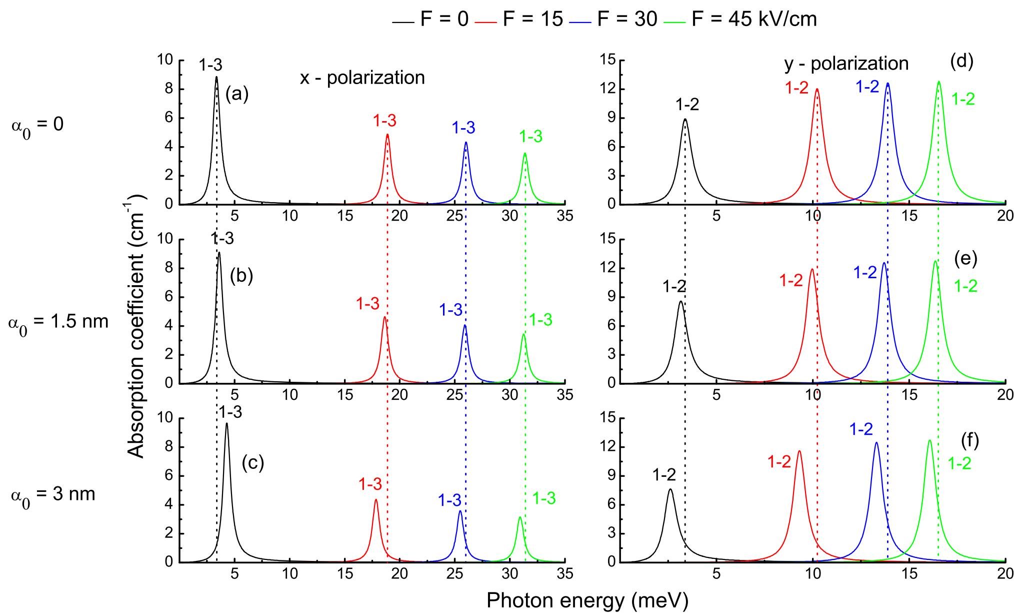

Figure 7. Dependence of the intraband optical absorption coefficient on incident photon energy in QR. The results are presented for $R_1 = 5$ nm and $R_2 = 25$ nm. Both x-and y-light polarizations are considered for several values of the laser field parameter α_0 and electric field strength F.

strength P_{fi} is expressed as follows [49]: $P_{fi} = 2\,m\hbar^{-2}e^{-2}\Delta E_{fi}|M_{fi}|^2$, where $\Delta E_{fi} = E_f - E_i$. As can be seen from the expression, the behavior of the oscillator strength depends on the energy difference and matrix element. Taking into account the importance of the mentioned physical quantities, the laser field parameter α_0 and electric field strength F dependent oscillator strengths are presented in figures 6(a) and (b), respectively. The sizes of the structure are fixed $R_1 = 5$ nm and $R_2 = 25$ nm and different incident light polarizations are considered. The inset figures of figure 6(a) and (b) show the absolute value of matrix elements of the allowed transitions as a function of laser field parameter and electric field strength, respectively. For nonzero values of α_0 and F different selection rules are obtained. In the case of x-polarization, transitions from the ground state $j = 1$ to the second excited state $j = 3$ are allowed (see red lines in figure 6) and in the case of y-polarization, the $1 \to 2$ transitions are allowed (see blue lines in figure 6).

The obtained selection rules can be explained as follows. Each time initial (i) and final (f) states have different, defined parity with respect to an axis, the transition matrix element will be non-zero for a light wave polarized on that axis

- for $\alpha_0 = 0$ and $F = 0$ (i) is even and (f) is odd no matter the polarization of the absorbed light; therefore, it is expected that the transition matrix element be non-zero and invariant to the light polarization, which is confirmed by the numerical calculation of the oscillator strength in figure 6(a) and the matrix elements in the inset;

- for $\alpha_0 > 0$ and $F = 0$ transition, $1 \to 2$ will be forbidden for x-polarization since Φ_d^1 and Φ_d^2 have the same parity (even) with respect to x variable so that the associated matrix element will be zero at all non-zero values of the laser parameter; similarly, transition $1 \to 3$ will be forbidden for y-polarization of the light, since Φ_d^1 and Φ_d^3 are both even functions of variable y; these remarks are confirmed by the numerical calculation of the matrix elements in the inset of figure 6(a);

- similarly, for $F > 0$ transitions, $1 \to 2$ (in the case of x -polarization) and $1 \to 3$ (in the case of y-polarization) are forbidden by the parities of the wave functions, as illustrated in the lower part of figure 5 and confirmed by the calculations in the inset of former figure 6(b).

The physics behind the behaviors of the matrix elements can be explained using the wave function distributions of corresponding states [50]: As can be seen from Figure5, with the increase of α_0, overlapping of $j = 1$ and $j = 2$ states decreases, while the overlapping of $j = 1$ and $j = 3$ states increases. Therefore, the matrix elements M_{12} and M_{13} augment and diminish, respectively. The opposite behavior has the oscillator strength of mentioned transitions, which can be explained by the simultaneous variations of energy difference and squared matrix elements.

In figure 7 we present the intraband optical absorption coefficient as a function of the incident photon energy for several values of the laser field parameter α_0 (figures 7(a)–(c)) and electric field strength (figures 7(d)–(f)). The sizes of the structure are fixed $R_1 = 5$ nm and $R_2 = 25$ nm and different incident light polarizations are considered. As can be seen from figure 7, the simultaneous influences of the intense laser field and lateral electric field result on the following effects in the intraband absorption spectrum:

1. In both cases of light polarization the increment of the electric field results in a blueshift in the intraband absorption spectrum, which is induced by the increment of the energy distances between the ground and both excited energy levels. On the other hand, in the case of x- polarization a decrease of

the peak value is observed, and in the case of y- polarization the peak value increases. These are the results of the increase and decrease of the oscillator strength (see figure 6 (b)) in the case of x- and y-polarizations, respectively.

2. If $F = 0$ the increasing of the laser field parameter the blueshift in the intraband absorption spectrum is observed in the case of x-polarization due to the increment of the energy distance between $j = 3$ and $j = 1$ states. Meanwhile, the strengthening of the laser field results in the decreases of the energy difference between the $j = 2$ and $j = 1$ states leading to the redshift in the absorption spectrum. On the other hand, in the case of $F \neq 0$ the increment of the laser field makes the redshifts in the spectrum, due to the decrease of the energy differences between the ground and both excited states. The variations of the peak values in different cases result from the appropriate behavior of the oscillator strength (see figure 6(a)).

4. Conclusions

We have studied the simultaneous influences of the ILF and lateral electric field on one-electron states in GaAs/$Ga_{0.7}Al_{0.3}$ As single QRs. Also, we have investigated the influence of the light polarization direction on the intraband absorption coefficient. We have observed the splitting and increasing of energy levels induced by the ILF. Meanwhile, the energy splitting, decreasing and increasing of energy levels induced by the lateral electric field were obtained. Our results show that the incident light polarization can induce redshifts and blueshifts in the intraband absorption spectrum of the QR. On the other hand, the simultaneous influences of the ILF and lateral electric field can lead both to the blueshift and redshift of the intraband optical absorption spectrum. To our knowledge this is the first systematic theoretical study of the simultaneous effects of the ILF and lateral electric field on the electronic and optical properties of ring-like nanostructures. Thereby, in our model calculations we have shown that by manipulating the laser field paramater and homogeneous electric field strength we can alter the overlap of the electron wave functions so that the transition probability will be enhanced or suppressed on demand. Thus, the basic issues of quantum mechanics can be explored to design new semiconductor QR devices in which specific properties can be optimized.

Acknowledgments

The work of AAK and MGB was supported by the Armenian State Committee of Science (Project nos. 13YR-1C0012 and AR-13RF-093). DL acknowledges partial financial support from EPSRC under grant: EP/L002922/1, FONDECYT 1120764, Millennium Scientific Initiative, P10–061-F, Basal Program Center for Development of Nanoscience and Nanotechnology (CEDENNA) and UTA-project 8750–12.

References

[1] Aharonov Y and Bohm D 1959 *Phys. Rev.* **115** 485

[2] Lorke A, Luyken R J, Govorov A O, Kotthaus J P, Garcia J M and Petroff P M 2000 *Phys. Rev. Lett.* **84** 2223

[3] Fuhrer A, Lüscher S, Ihn T, Heinzel T, Ensslin K, Wegscheider W and Bichler M 2001 *Nature* **413** 822

[4] Lee B C, Voskoboynikov O and Lee C P 2004 *Physica* E **24** 87

[5] Fomin V M 2014 *Physics of Quantum Rings* (Berlin: Springer)

[6] Bayer M, Korkusinski M, Hawrylak P, Gutbrod T, Michel M and Forchel A 2003 *Phys. Rev. Lett.* **90** 186801

[7] Cui J, He Q, Jiang X M, Fan Y L, Yang X J, Xue F and Jiang Z M 2003 *Appl. Phys. Lett.* **83** 2907

[8] Huang G, Guo W, Bhattacharya P, Ariyawansa G and Perera A G U 2009 *Appl. Phys. Lett.* **94** 101115

[9] Wu J, Wang Z M, Dorogan V G, Li S, Zhou Z, Li H, Lee J, Kim E S, Mazur Y I and Salamo G J 2012 *Appl. Phys. Lett.* **101** 043904

[10] Young R J, Smakman E P, Sanchez A M, Hodgson P, Koenraad P M and Hayne M 2012 *Appl. Phys. Lett.* **100** 082104

[11] Abbarchi M, Mastrandrea C, Vinattieri A, Sanguinetti S, Mano T, Kuroda T, Koguchi N, Sakoda K and Gurioli M 2009 *Phys. Rev.* B **79** 085308

[12] Zipper E, Kurpas M, Sadowski J and Maska M M 2011 *J. Phys.: Condens. Matter* **23** 115302

[13] Ganichev S D and Prettl W 2006 *Intense Terahertz Excitation of Semiconductors* (Oxford: Oxford University Press)

[14] Markelz A G, Asmar N G, Brar B and Gwinn E G 1996 *Appl. Phys. Lett.* **69** 3975

[15] Mori N, Takahashi T, Kambayashi T, Kubo H, Hamaguchi C, Eaves L, Foxon C T, Patane A and Henini M 2002 *Phys.* B **314** 431

[16] Asmar N G, Markelz A G, Gwinn E G, Cerne J, Sherwin M S, Chapman K L, Hopkins P E and Gossard A C 1995 *Phys. Rev.* B **51** 18041

[17] Hughes S and Citrin D S 2000 *Phys. Rev. Lett.* **84** 4228

[18] Hsu H and Reichl L E 2006 *Phys. Rev.* B **74** 115406

[19] Ozturk E, Sari H and Sökmen I 2005 *J. Phys. D: Appl. Phys.* **38** 935

[20] Kasapoglu E and Sökmen I 2008 *Physica* B **403** 3746

[21] Karabulut İ 2010 *Appl. Surf. Sci.* **256** 7570

[22] Xia C, Zhu Y and Wei S 2011 *Phys. Lett.* A **375** 2652

[23] Mora-Ramos M E, Duque C A, Kasapoglu E, Sari H and Sökmen I 2012 *J. Lumin.* **132** 901

[24] Ungan F, Yesilgul U, Sakiroglu S, Kasapoglu E, Sari H and Sökmen I 2013 *J. Lumin.* **143** 75

[25] Yesilgul U, Ungan F, Sakiroglu S, Mora-Ramos M E, Duque C A, Kasapoglu E, Sari H and Sökmen I 2014 *J. Lumin.* **145** 379

[26] Kasapoglu E, Sari H, Yesilgul U and Sokmen I 2006 *J. Phys.: Condens. Matter.* **18** 6263

[27] Safarpour G, Izadi M A, Niknam E, Moradi M and Golshan M M 2014 *Physica B* **436** 14

[28] Duque C A, Kasapoglu E, Sakiroglu S, Sari H and Sökmen I 2010 *Appl. Surf. Sci.* **256** 7406

[29] Burileanu L M 2014 *J. Lumin.* **145** 684

[30] Niculescu E C, Cristea M and Radu A 2014 *Superlattices Microstruct.* **69** 65

[31] Radu A, Kirakosyan A A, Laroze D, Baghramyan H M and Barseghyan M G 2014 *J. Appl. Phys.* **116** 093101

[32] Farias G A, Degani M H, Freire J A K, Costa e Silva J and Ferreira R 2008 *Phys. Rev.* B **77** 085316

[33] Chakraborty T 2003 *Adv. Solid State Phys.* **43** 79

[34] Fanyao Q, Fonseca A L A and Nunes O A C 1996 *Phys. Rev.* B **54** 16405

[35] Niculescu E C, Burileanu L M, Radu A and Lupaşcu A 2011 *J. Lumin.* **131** 1113

[36] Fanyao Q and Morais P C 2003 *Phys. Lett.* A **310** 460
[37] Burileanu L M and Radu A 2011 *Opt. Commun.* **284** 2050
[38] Barseghyan M G, Duque C A, Niculescu E C and Radu A 2014 *Superlattices Microstruct.* **66** 10
[39] Manaselyan A K, Barseghyan M G, Kirakosyan A A, Laroze D and Duque C A 2014 *Physica* E **60** 95
[40] Gangopadhyay S and Nag B R 1996 *Phys. Status Solidi b* **195** 123
[41] Tiutiunnyk A, Tulupenko V, Mora-Ramos M E, Kasapoglu E, Ungan F, Sari H, Sökmen I and Duque C A 2014 *Physica* E **60** 127
[42] Kasapoglu E, Ungan F, Sari H, Sökmen I, Mora-Ramos M E and Duque C A 2014 *Superlattices Microstruct.* **73** 171
[43] Şahin M and Köksal K 2012 *Semicond. Sci. Technol.* **27** 125011
[44] Alexeev A M and Portnoi M E 2012 *Phys. Rev.* B **85** 245419
[45] Yu P Y and Cardona M 1996 *Fundamentals of Semiconductors* (Berlin: Springer)
[46] Niculescu E C and Radu A 2011 *Eur. Phys. J.* B **80** 73
[47] Bloss W L 1989 *J. Appl. Phys.* **65** 4789
[48] Miller D A B, Chemla D S and Damen T C 1984 *Phys. Rev. Lett.* **53** 2173
[49] Liang S, Xie W, Sarkisyan H A, Meliksetyan A V and Shen H 2011 *J. Phys.: Condens. Matter* **23** 415302
[50] Iotti R C and Andreani L C 1997 *Phys. Rev.* B **56** 3922